

A POSTERIORI ERROR ESTIMATION FOR A SINGULARLY PERTURBED PROBLEM WITH TWO SMALL PARAMETERS

TORSTEN LINSS

Abstract. A singularly perturbed two-point boundary-value problem of reaction-convection-diffusion type is considered. The problem involves two small parameters that give rise to two boundary layers of different widths. The problem is solved using a streamline-diffusion FEM (SDFEM).

A robust *a posteriori* error estimate in the maximum norm is derived. It provides computable and guaranteed upper bounds for the discretisation error. Numerical examples are given that illustrate the theoretical findings and verify the efficiency of the error estimator on *a priori* adapted meshes and in an adaptive mesh movement algorithm.

Key Words. reaction-convection-diffusion problems, finite element methods, a posteriori error estimation, singular perturbation

1. Introduction

Consider the reaction-convection-diffusion problem of finding $u \in C^2(0, 1) \cap C[0, 1]$ such that

$$(1) \quad \mathcal{L}u := -\varepsilon_d u'' - \varepsilon_c b u' + cu = f \text{ in } (0, 1) \quad \text{and} \quad u(0) = u(1) = 0,$$

where $\varepsilon_d \in (0, 1]$ and $\varepsilon_c \in [0, 1]$ are small parameters, while $b \in C^1(0, 1)$ and $c, f \in C(0, 1)$ are assumed to satisfy

$$(2) \quad b \geq 1, \quad c \geq 1 \quad \text{and} \quad \varepsilon_c b' + c \geq 0 \text{ in } (0, 1).$$

The positivity of b and c is essential, while the third inequality merely provides a maximal threshold value for ε_c for which the analysis in the paper is valid.

The standard weak formulation of (1) is: Find $u \in H_0^1(0, 1)$ such that

$$(1') \quad a(u, v) := \varepsilon_d (u', v') - \varepsilon_c (b u', v) + (cu, v) = (f, v) =: f(v) \quad \forall v \in H_0^1(0, 1).$$

The solution of (1) typically exhibits two boundary layers of different widths at the two endpoints of the domain. Because of the presence of these layers standard numerical methods fail to give accurate approximations. Unless a prohibitively large number of mesh points is used, the layers are not resolved, and the rate of convergence achieved by the method is far less than that obtain in the non-singularly perturbed case.

The goal is to construct so-called *robust* or *uniformly convergent* methods. This means that for a fixed number of mesh points, the accuracy and rate of convergence is guaranteed, irrespective of the magnitude of the perturbation parameters. Approaches for achieving this aim include the use of meshes that contain a concentration of points in the region of the boundary layers. The piecewise uniform meshes of Shishkin [18], and the graded meshes of Bakhvalov [2] are examples of

such. The construction of these meshes depends strongly on *a priori* information of the solution and its derivatives.

Adapted numerical methods for (1) were first analysed by Shishkin and Titov [22]. They consider an exponentially fitted finite difference scheme on a uniform mesh. This method is shown to be convergent, uniformly in the parameters ε_d and ε_c , in the discrete maximum norm. The order of convergence is at least $N^{-2/5}$, where N is the number of mesh intervals.

About 25 years after the work by Shishkin and Titov a number of authors started to investigate standard numerical methods on special layer-adapted meshes. Linß and Roos [17] studied a first-order upwinded difference scheme on a piecewise uniform Shishkin mesh. Uniform convergence of $\mathcal{O}(N^{-1} \ln N)$ was established. A theory for this method on general meshes was developed in [14].

Second-order upwind schemes were considered by Roos and Uzelac [21] (using a SDFEM approach) and by Gracia et al. [8]. Both papers establish uniform convergence of $\mathcal{O}(N^{-2} \ln^2 N)$ on Shishkin meshes.

While these *a priori* results establish the asymptotic behaviour of the error as the mesh is refined, it cannot give guaranteed upper bounds for the error on a particular mesh. The constant in the error bound, though independent of the perturbation parameters, depends on the exact solution u which in turn is unknown.

The main contribution of the present study is in establishing *a posteriori* error bounds which provide upper bounds on the error of the SDFEM. These days, *a posteriori* error estimates for classical problems, i.e. problems that are not singularly perturbed, are well established, see for example the monographs [1] and [23]. Results are also available for the SDFEM applied to convection-diffusion problems [24]. All these analyses are set in an L_2 - and energy-norm framework. However, for (1) these norms fail to capture the layers. Therefore, we are interested in *maximum-norm* error bounds.

For singularly perturbed problems, *a posteriori* error analyses in the maximum norm have been pioneered by Kopteva both for convection-diffusion problems in 1D [10] and for reaction-diffusion problems in 1-3D [11, 12, 7]. In the present paper, *a posteriori* error bounds for a single equation with two independently small parameters are derived for the first time. In a certain sense it generalises the 1D results by Kopteva for both reaction-diffusion ($\varepsilon_c = 0$) and convection-diffusion ($\varepsilon_c = 1$).

Outline. The paper is organised as follows. In § 2 we study properties of the continuous problem (1). In particular bounds for the Greens function associated with \mathcal{L} are derived that are essential in the later error analysis. The SDFEM for (1') is introduced in § 3, while § 4 is devoted to its *a posteriori* error analysis. An adaptive mesh movement algorithm is adapted from the literature in § 5. The article closes with results of some numerical experiments.

Notation. Throughout C denotes a generic positive constant that is independent of the parameters ε_d and ε_c and of N , the number of mesh points. We use $\|\cdot\|_D$ to denote the norm in $L_\infty(D)$. When $D = (0, 1)$ we drop the D from the notation.

2. Properties of the continuous problem

The solution of (1) and its Green's function can be described by means of the two roots of the characteristic equation

$$(3) \quad -\varepsilon_d \lambda(x)^2 - \varepsilon_c b(x) \lambda(x) + c(x) = 0.$$

This quadratic equation defines two continuous functions $\lambda_i : [0, 1] \rightarrow \mathbb{R}$ with $\lambda_0 < 0$ and $\lambda_1 > 0$ on $[0, 1]$:

$$\lambda_{0,1}(x) = -\frac{1}{2\varepsilon_d} \left(\varepsilon_c b(x) \pm \sqrt{4\varepsilon_d c(x) + \varepsilon_c^2 b(x)^2} \right).$$

The quantity λ_0 describes the boundary layer at $x = 0$, while λ_1 characterises the layer at $x = 1$. Set

$$\mu_0 := \max_{x \in [0,1]} \lambda_0(x) < 0 \quad \text{and} \quad \mu_1 := \min_{x \in [0,1]} \lambda_1(x) > 0.$$

There are essentially three regimes:

		$ \mu_0 $	μ_1
convection-diffusion	$\varepsilon_d \ll \varepsilon_c = 1$	$\mathcal{O}(\varepsilon_d^{-1})$	$\mathcal{O}(1)$
reaction-convection-diffusion	$\varepsilon_d \ll \varepsilon_c^2 \ll 1$	$\mathcal{O}(\varepsilon_c \varepsilon_d^{-1})$	$\mathcal{O}(\varepsilon_c^{-1})$
reaction-diffusion	$\varepsilon_c^2 \ll \varepsilon_d \ll 1$	$\mathcal{O}(\varepsilon_d^{-1/2})$	$\mathcal{O}(\varepsilon_d^{-1/2})$

Remark 1. The values of λ_0 and λ_1 do not vary significantly on $[0, 1]$ because

$$(4) \quad \frac{\lambda_1(\xi)}{\lambda_1(\eta)} = \frac{c(\xi)\lambda_0(\eta)}{c(\eta)\lambda_0(\xi)} \geq \begin{cases} \|b\|_\infty^{-1} \|c\|_\infty^{-1} & \text{if } \varepsilon_c > 0, \\ \|c\|_\infty^{-1/2} & \text{if } \varepsilon_c = 0, \end{cases}$$

for all $\xi, \eta \in [0, 1]$.

2.1. Derivative bounds and layer-adapted meshes. Bounds on derivatives of the exact solution are essential to conduct *a priori* error analyses of numerical methods. They are also required when designing layer-adapted meshes. The following result from [17] provides this information.

Lemma 1. Let $b, c, f \in C^q[0, 1]$ for some $q \in \mathbb{N}^+$. Let $p \in (0, 1)$ be arbitrary, but fixed. Assume $q\|b'\|_{\varepsilon_c} < 1 - p$. Then

$$\left| u^{(k)}(x) \right| \leq C \left\{ 1 + (-\mu_0)^k e^{p\mu_0 x} + \mu_1^k e^{-p\mu_1(1-x)} \right\}, \quad \text{for } x \in (0, 1)$$

and $k = 0, \dots, q$.

Remark 2. Different derivative bounds are given in [8] and [21]. They can be recovered from Lemma 1.

This information about the layer structure can be used to design layer-adapted meshes *a priori*; see [15]. Let us consider two frequently used types of meshes.

Bakhvalov meshes [2] concentrate mesh points inside the layer by using a mesh generating function which is essentially the inverse of the layer function. Choosing mesh parameters $K_0, K_1 > 0$ and $\sigma_0, \sigma_1 > 0$, Bakhvalov meshes for (1) can be generated by equidistributing the monitor function

$$M_{Ba}(s) := \max \left\{ 1, \frac{K_0 |\mu_0|}{\sigma_0} e^{\mu_0 s / \sigma_0}, \frac{K_1 \mu_1}{\sigma_1} e^{-\mu_1(1-s) / \sigma_1} \right\},$$

i.e. the mesh points $x_i, i = 0, \dots, N$, are chosen such that

$$(5) \quad \int_{x_{i-1}}^{x_i} M_{Ba}(s) ds = N^{-1} \int_0^1 M_{Ba}(s) ds.$$

Fig. 1 depicts a Bakhvalov mesh with 16 mesh intervals for (1).

The parameters σ_0 and σ_1 determine the stretching of the mesh inside the layer. They must be chosen greater or equal to the formal order of the scheme used. The parameter K_0 and K_1 determine the portion of mesh points used to resolve the

layers. About $NK_0/(1 + K_0 + K_1)$ mesh points are placed inside the layer at $x = 0$, and $NK_1/(1 + K_0 + K_1)$ mesh points near $x = 1$.

Note that (5) is equivalent to

$$\int_0^{x_i} M_{Ba}(s) \, ds = \frac{i}{N} \int_0^1 M_{Ba}(s) \, ds, \quad i = 0, \dots, N,$$

from which explicit formulae for the mesh points $x_i, i = 0, \dots, N$, can be derived by evaluating the integrals involved and solving for x_i .

Bakhvalov’s original construction in [2] for a reaction-diffusion problem with two layers of equal widths is geometric. The characterisation by means of equidistribution is equivalent and easily extends to more complicated layer structures, in particular when overlapping layers occur; see [15].

Shishkin meshes [18] are piecewise uniform. Fixing mesh parameters $q_0, q_1 > 0$ and $\sigma_0, \sigma_1 > 0$ with $q_0 + q_1 < 1$, we define the mesh transition points

$$\tau_0 = \min \left\{ q_0, \frac{\sigma_0}{|\mu_0|} \ln N \right\} \quad \text{and} \quad \tau_1 = \min \left\{ q_1, \frac{\sigma_1}{\mu_1} \ln N \right\}.$$

Then the intervals $[0, \tau_0]$ and $[1 - \tau_1, 1]$ are dissected into q_0N and q_1N subintervals, while $[\tau_0, 1 - \tau_1]$ is divided into $(1 - q_0 - q_1)N$ subintervals; see Fig. 1 for a sketch. Usually $\sigma_0 = \sigma_1$ and $q_0 = q_1 = 1/4$ are considered in the literature.

Again, the parameters σ_0 and σ_1 must be chosen equal to the formal order of the numerical method used (or greater). Note, when $\tau_0 = \sigma_0 |\mu_0|^{-1} \ln N$, then $e^{\mu_0 \tau_0} = N^{-\sigma_0}$. Thus, on $[\tau_0, 1]$ the magnitude of the layer term $e^{\mu_0 x}$ has decayed to the order of the method.

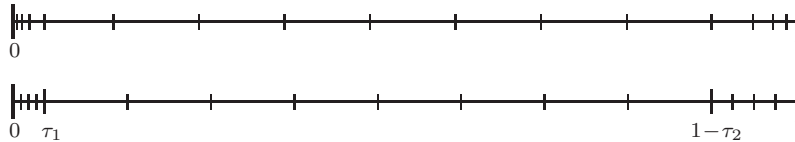


FIGURE 1. Bakhvalov mesh (top) and Shishkin mesh (below) for a reaction-convection-diffusion equation. The layers at $x = 0$ and $x = 1$ have different widths.

2.2. Stability and Green’s function estimates. By means of the Green’s function $\mathcal{G} : [0, 1]^2 \rightarrow \mathbb{R}$ any function $v \in H_0^1(0, 1)$ can be represented as

$$(6) \quad v(x) = a(v, \mathcal{G}(x, \cdot)) \quad \text{for } x \in (0, 1).$$

In turn (6) can be regarded as defining the Green’s function: For fixed $x \in (0, 1)$ find $\mathcal{G}(x, \cdot) \in H_0^1(0, 1)$ such that (6) is satisfied for all $v \in H_0^1(0, 1)$. Using the differential operator \mathcal{L} , we may seek, for fixed $\xi \in (0, 1)$, $\mathcal{G}(\cdot, \xi)$ such that

$$(\mathcal{L}\mathcal{G}(\cdot, \xi))(x) = \delta(x - \xi) \quad \text{for } x \in (0, 1), \quad \mathcal{G}(0, \xi) = \mathcal{G}(1, \xi) = 0,$$

while for fixed $x \in (0, 1)$ we have

$$(7) \quad (\mathcal{L}^*\mathcal{G}(x, \cdot))(\xi) = \delta(\xi - x) \quad \text{for } \xi \in (0, 1), \quad \mathcal{G}(x, 0) = \mathcal{G}(x, 1) = 0,$$

with the adjointed operator

$$\mathcal{L}^*v = -\varepsilon_d v'' + \varepsilon_c (bv)' + cv.$$

Fig. 2 depicts typical plots of the graph of $\mathcal{G}(x, \cdot)$. It is non-negative, has a maximum of order $\mathcal{O}(\mu_1)$ at $x = \xi$. It is monotonically increasing for $\xi < x$, but decreasing for $\xi > x$. These properties will be rigorously proved now. Thereby, we generalise the Green's-function bounds by Kopteva for both convection-diffusion [10] and for reaction-diffusion problems [11]. We do so by carefully analysing the dependence of the Green's function on the parameter ε_c .

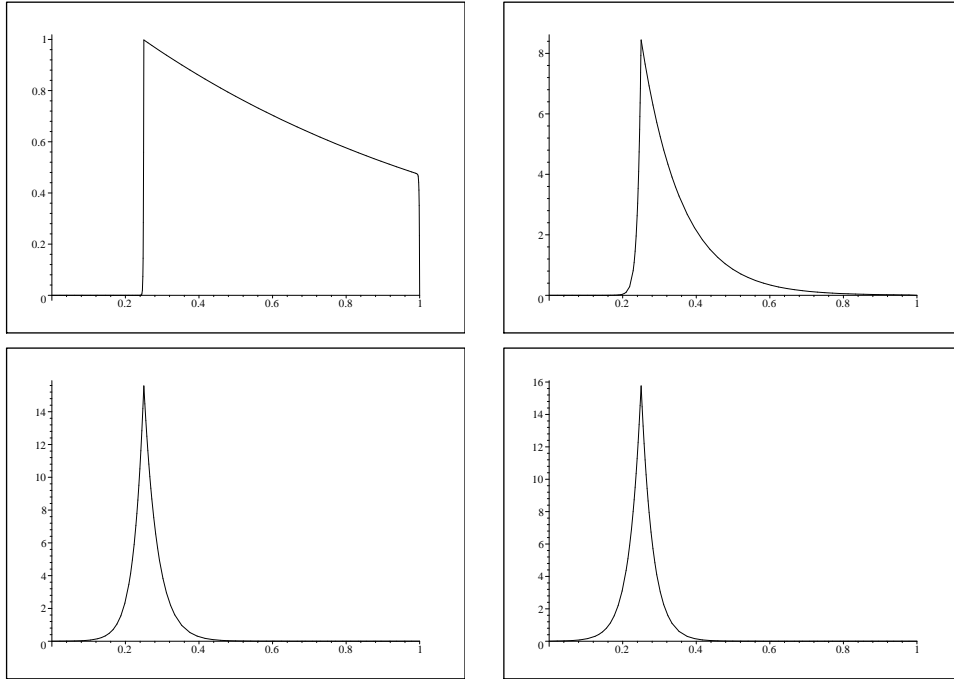


FIGURE 2. Green's function $\mathcal{G}(x, \cdot)$ associated with \mathcal{L} ; $\varepsilon_d = 10^{-3}$, $\varepsilon_c = 1, 10^{-1}, 10^{-2}, 0$ (from left to right).

Lemma 2. *Let $\xi \in (0, 1)$ be arbitrary, but fixed. Then for any two functions $v, w \in C[0, 1] \cap C^2((0, \xi) \cup (\xi, 1))$*

$$\left. \begin{aligned} \mathcal{L}v &\leq \mathcal{L}w \quad \text{in } (0, 1) \setminus \{\xi\} \\ v(0) &\leq w(0) \\ v(1) &\leq w(1) \\ -[v'](\xi) &\leq -[w'](\xi) \end{aligned} \right\} \implies v \leq w \quad \text{on } [0, 1].$$

Proof. The proof is by contradiction and follows standard arguments for maximum principles, cf. [19]. The crucial point is the strict positivity of the reaction coefficient c . □

Lemma 3. *For $i = 0, 1$ and all $x \in [0, 1]$*

$$-\varepsilon_d \mu_i^2 - \varepsilon_c b(x) \mu_i + c(x) \geq 0.$$

Proof. (i) We consider $i = 0$ first. Let $x \in [0, 1]$ be arbitrary

$$-\varepsilon_d \mu_0^2 - \varepsilon_c b(x) \mu_0 \geq \mu_0 (-\varepsilon_d \lambda_0(x) - \varepsilon_c b(x))$$

because $0 > \mu_0 \geq \lambda_0(x)$ for all $x \in [0, 1]$. The characteristic equation (3) yields

$$-\varepsilon_d \mu_0^2 - \varepsilon_c b(x) \mu_0 \geq -\mu_0 \lambda_0(x)^{-1} c(x)$$

Using $c(x) \geq 1$ and $\lambda_0(x) \leq \mu_0 < 0$ again, completes the proof for μ_0 .

(ii) Now study μ_1 .

$$-\varepsilon_d \mu_1^2 - \varepsilon_c b(x) \mu_1 \geq -\varepsilon_d \lambda_1(x)^2 - \varepsilon_c b(x) \lambda_1(x)$$

because $0 < \mu_1 \leq \lambda_1(x)$ for all $x \in [0, 1]$. Using the characteristic equation (3), we are done. \square

Theorem 1. *Suppose (2) holds. Then the Green's function \mathcal{G} associated with \mathcal{L} satisfies the pointwise bounds*

$$0 \leq \mathcal{G}(x, \xi) \leq \bar{\mathcal{G}}(x, \xi) := \frac{1}{\varepsilon_d (\mu_1 - \mu_0)} \begin{cases} e^{\mu_1(x-\xi)} & \text{for } 0 \leq x \leq \xi \leq 1, \\ e^{\mu_0(x-\xi)} & \text{for } 0 \leq \xi \leq x \leq 1 \end{cases}$$

and

$$\begin{aligned} \mathcal{G}_\xi(x, \xi) &\geq 0 && \text{for } 0 \leq \xi < x \leq 1, \\ \mathcal{G}_\xi(x, \xi) &\leq 0 && \text{for } 0 \leq x < \xi \leq 1. \end{aligned}$$

Furthermore we have the L_1 -norm bounds

$$(8) \quad \int_0^1 c(\xi) \mathcal{G}(x, \xi) \, d\xi \leq 1.$$

and

$$\int_0^1 |\mathcal{G}_\xi(x, \xi)| \, d\xi \leq \frac{2}{\varepsilon_d (\mu_1 - \mu_0)}$$

and

$$\varepsilon_d \int_0^1 |\mathcal{G}_{\xi\xi}(x, \xi)| \, d\xi \leq \varepsilon_c \left\{ \frac{2\|b\|}{\varepsilon_d (\mu_1 - \mu_0)} + \left\| \frac{b'}{c} \right\| \right\} + 2 =: \gamma^*.$$

Proof. (i) Using Lemma 2 one verifies that $0 \leq \mathcal{G}$ on $[0, 1]^2$.

Lemma 3 gives $\mathcal{L}\bar{\mathcal{G}}(\cdot, \xi) \geq 0$ on $(0, 1) \setminus \{\xi\}$. Clearly $\bar{\mathcal{G}}(0, \xi) > 0$ and $\bar{\mathcal{G}}(1, \xi) > 0$. The jump of $\bar{\mathcal{G}}_x$ satisfies $-\varepsilon_d [\bar{\mathcal{G}}_x(\cdot, \xi)](\xi) = 1$. Application of Lemma 2 establishes the upper bound on \mathcal{G} .

Because $\mathcal{G}(x, 0) = \mathcal{G}(x, 1) = 0$ for $x \in [0, 1]$ and $\mathcal{G} \geq 0$ on $[0, 1]^2$ we have

$$(9) \quad \mathcal{G}_\xi(x, 0) \geq 0 \quad \text{and} \quad \mathcal{G}_\xi(x, 1) \leq 0 \quad \text{for } x \in [0, 1].$$

Integrate (7) over $[0, 1]$ to obtain

$$-\varepsilon_d (\mathcal{G}_\xi(x, 1) - \mathcal{G}_\xi(x, 0)) + \int_0^1 c(\xi) \mathcal{G}(x, \xi) \, d\xi = 1.$$

By (9) we get (8).

(ii) Next we prove the monotonicity of $\mathcal{G}(x, \cdot)$. Integrating (7) over $[0, \xi]$, we get

$$-\varepsilon_d (\mathcal{G}_\xi(x, \xi) - \mathcal{G}_\xi(x, 0)) + \varepsilon_c b(\xi) \mathcal{G}(x, \xi) = - \int_0^\xi c(s) \mathcal{G}(x, s) \, ds \leq 0$$

for $\xi < x$. Thus

$$\varepsilon_d \mathcal{G}_\xi(x, \xi) \geq \varepsilon_d \mathcal{G}_\xi(x, 0) + \varepsilon_c b(\xi) \mathcal{G}(x, \xi) \geq 0 \quad \text{for } \xi < x$$

because $\mathcal{G}(x, \xi) \geq 0$ and $\mathcal{G}_\xi(x, 0) \geq 0$.

On the other hand, inspecting the differential equation (7), we see that $v = \mathcal{G}_\xi(x, \cdot)$ satisfies

$$-\varepsilon_d v' + \varepsilon_c b v = -(\varepsilon_c b' + c) \mathcal{G} \leq 0 \quad \text{in } (\xi, 1) \quad \text{and} \quad v(1) \leq 0,$$

if $\varepsilon_c b' + c$ is assumed to be positive. Application of a maximum principle for first-order operators yields $v \leq 0$ on $[x, 1]$.

Finally, for fixed $x \in (0, 1)$,

$$\int_0^1 |\mathcal{G}_\xi(x, \xi)| \, d\xi = \int_0^x \mathcal{G}_\xi(x, \xi) \, d\xi - \int_0^x \mathcal{G}_\xi(x, \xi) \, d\xi = 2\mathcal{G}(x, x)$$

because of the sign of \mathcal{G}_ξ . Recalling the first proposition of the theorem, we get the L^1 -norm bound on \mathcal{G}_ξ .

The last inequality of the theorem follows upon integrating (7) and using the bound for \mathcal{G} and \mathcal{G}_ξ established before. \square

Remark 3. *The function $\bar{\mathcal{G}}$ attains its maximum for $x = \xi$. Because λ_0 is continuous there exists a $x^* \in [0, 1]$ with $\lambda_0(x^*) = \mu_0$. Therefore*

$$\frac{1}{\varepsilon_d(\mu_1 - \mu_0)} \leq -\frac{1}{\varepsilon_d \lambda_0(x^*)} = \frac{\lambda_1(x^*)}{c(x^*)} \leq C\mu_1, \quad \text{by (4).}$$

If $\varepsilon_c = 0$ this estimate can be sharpened to

$$\frac{1}{\varepsilon_d(\mu_1 - \mu_0)} \leq \frac{\mu_1}{2} \leq \frac{1}{2\sqrt{\varepsilon_d}}$$

since $\mu_1 = -\mu_0 \leq 1/\sqrt{\varepsilon_d}$.

3. Discretisation

Starting from the weak formulation (1') we shall consider finite-element discretisations with piecewise linear trial and test functions. Let $\bar{\omega}_N : 0 = x_0 < x_1 < \dots < x_N = 1$ be an arbitrary mesh on $[0, 1]$ with N mesh intervals $I_i = (x_{i-1}, x_i)$ of length $h_i := x_i - x_{i-1}$. Set $V^N = \mathcal{S}_1^0(\bar{\omega}_N) \cap H_0^1(0, 1)$, where

$$\mathcal{S}_1^0(\bar{\omega}_N) := \left\{ v \in C[0, 1] : v|_{I_i} \in \Pi_1 \text{ for } i = 0, \dots, N-1 \right\}$$

denotes the space of piecewise linear continuous splines.

A standard FEM approximation for (1') is: Find $u^N \in V^N$ such that

$$a(u^N, v^N) = f(v^N) \quad \forall v^N \in V^N.$$

Typically the integrals involved in this discretisation cannot be evaluated exactly and have to be approximated using quadrature. Special quadrature rules will give different FEM methods.

Here we shall consider the following unstabilised FEM. Find $u^N \in V^N$ such that

$$(10) \quad a_{FE}(u^N, v^N) = f_{FE}(v^N) \quad \text{for all } v^N \in V^N$$

with

$$a_{FE}(w, v) := \varepsilon_d(w', v') + ((-\varepsilon_c b w' + c w)^I, v) \quad \text{and} \quad f_{FE}(v) := (f^I, v).$$

Here (\cdot, \cdot) is the standard L_2 scalar product and φ^I is the piecewise linear interpolant of φ , i.e., that function $\varphi^I \in \mathcal{S}_1^0(\bar{\omega}_N)$ with $\varphi^I(x_i) = \varphi(x_i)$ for $i = 0, \dots, N$.

It is well known that for singularly perturbed problems stabilisation is essential. We follow Hughes and Brooks [9] and use streamline-diffusion stabilisation, i.e. we add weighted residuals to (1'):

$$(11) \quad a(u, v) - \sum_{i=1}^N \tau_i (\mathcal{L}u - f, \varepsilon_c v')_{I_i} = f(v).$$

Here $(\cdot, \cdot)_D$ indicates that integration is restricted to D . The parameters $\tau_i \geq 0$, $i = 1, \dots, N$, are user chosen and will be fixed later. This kind of stabilisation

is consistent with (1') because if the solution of (1') is in $H^2(0,1)$ then it also solves (11).

Again, integrals have to be approximated by quadrature. Using the interpolation idea above we arrive at the following discretisation. Find $u^N \in V^N$ such that

$$(12) \quad a_{SD}(u^N, v^N) = f_{SD}(v^N) \quad \forall v^N \in V^N$$

where

$$a_{SD}(w, v) := a_{FE}(w, v) + \varepsilon_c \sum_{i=1}^N \tau_i ((\varepsilon_c b w' - c w)^I, v')_{I_i}$$

and

$$f_{SD}(v) := f_{FE}(v) - \varepsilon_c \sum_{i=1}^N \tau_i (f^I, v')_{I_i}.$$

Note that $w'' \equiv 0$ in $I_i, i = 1, \dots, N$, for $w \in V^N$.

4. A posteriori error analysis

The analysis starts from the representation (6). It is similar to that in [16] for a reaction-diffusion problem, but the presence of a convection term and also of extra stabilisation terms complicates the analysis. The analysis in [10] deals with a convection term too, but in the context of difference schemes. Moreover, in [10] the $W^{1,1}$ norm of the Green's function is uniformly bounded, because therein the special case $\varepsilon_c = 1$ is considered. For the two-parameter problem considered here, the $W^{1,1}$ norm of \mathcal{G} depends on negative powers of the perturbation parameters. This requires extra attention.

We consider the SDFEM (12). (Results for the unstabilised FEM (10) can be obtained by setting all $\tau_i = 0$.) Fix $x \in (0, 1)$ and set $\Gamma := \mathcal{G}(x, \cdot)$. By (1'),

$$(13) \quad (u - u^N)(x) = a(u - u^N, \Gamma) = f(\Gamma) - a(u^N, \Gamma) = -\varepsilon_d ((u^N)', \Gamma') + (q, \Gamma),$$

where here and throughout the remainder of the paper

$$(14) \quad q := f - c u^N + \varepsilon_c b (u^N)'$$

Clearly q may have discontinuities at the mesh points because $u^N \in \mathcal{S}_1^0$. Therefore we set

$$q_i^+ = \lim_{x \downarrow x_i} q(x) \quad \text{and} \quad q_i^- = \lim_{x \uparrow x_i} q(x)$$

for all mesh nodes x_i . Furthermore, let $q_{i-1/2}$ denote the value of q in the midpoint of I_i .

On the other hand, by (12),

$$\begin{aligned} 0 &= a_{SD}(u^N, \Gamma^I) - f_{SD}(\Gamma^I) \\ &= \varepsilon_d ((u^N)', (\Gamma^I)') - (q^I, \Gamma^I) + \varepsilon_c \sum_{i=1}^N \tau_i (q^I, (\Gamma^I)')_{I_i}. \end{aligned}$$

Adding this equation to (13), we get a general representation for the error:

$$(15) \quad (u - u^N)(x) = (q - q^I, \Gamma) + (q^I, \Gamma - \Gamma^I) + \varepsilon_c \sum_{i=1}^N \tau_i (q^I, (\Gamma^I)')_{I_i}.$$

The three terms on the right-hand side will be bounded separately. We shall restrict ourselves to the case $\varepsilon_c > 0$. The reaction-diffusion case $\varepsilon_c = 0$ was studied in [11, 16].

(i). A Hölder inequality gives

$$(16) \quad |(q - q^I, \Gamma)| \leq \|q - q^I\| = \max_{i=1, \dots, N} \|q - q^I\|_{I_i},$$

because $\|\Gamma\|_1 \leq 1$ by (8).

(ii). Consider the second term in (15). Again a Hölder inequality gives

$$\left| (q^I, \Gamma - \Gamma^I)_{I_i} \right| \leq \|q^I\|_{I_i} \|\Gamma - \Gamma^I\|_{1, I_i}.$$

We have

$$\|\Gamma - \Gamma^I\|_{1, I_i} \leq \frac{h_i}{2} \|\Gamma'\|_{1, I_i}$$

and

$$\|\Gamma - \Gamma^I\|_{1, I_i} \leq \frac{h_i^2}{8} \|\Gamma''\|_{1, I_i} = \frac{h_i^2}{8\varepsilon_d} \|\varepsilon_c (b\Gamma)' + c\Gamma - \delta(x - \cdot)\|_{1, I_i} \leq \frac{h_i^2}{8\varepsilon_d} N_i$$

with

$$N_i := \varepsilon_c \|b\|_{I_i} \|\Gamma'\|_{1, I_i} + \|(\varepsilon_c b' + c)\Gamma\|_{1, I_i} + \|\delta(x - \cdot)\|_{1, I_i}.$$

Hence

$$\left| (q^I, \Gamma - \Gamma^I)_{I_i} \right| \leq \|q^I\|_{I_i} \min \left\{ \frac{h_i^2}{8\varepsilon_d}, \frac{h_i}{2\varepsilon_c \|b\|_{I_i}} \right\} N_i,$$

because $\varepsilon_c \|b\|_{I_i} \|\Gamma'\|_{1, I_i} \leq N_i$.

Summing for $i = 1, \dots, N$ and using Theorem 1, we obtain

$$(17) \quad |(q^I, \Gamma - \Gamma^I)| \leq \gamma^* \max_{i=1, \dots, N} \left[\|q^I\|_{I_i} \min \left\{ \frac{h_i^2}{8\varepsilon_d}, \frac{h_i}{2\varepsilon_c \|b\|_{I_i}} \right\} \right].$$

Note γ^* was defined in Theorem 1.

(iii). Finally, we bound the last term in (15). Note that $(\Gamma^I)'$ is constant on each I_i . Therefore $\|(\Gamma^I)'\|_{1, I_i} \leq \|\Gamma'\|_{1, I_i}$ and

$$(18) \quad \varepsilon_c \left| \sum_{i=1}^N \tau_i (q^I, (\Gamma^I)')_{I_i} \right| \leq \varepsilon_c \sum_{i=1}^N \tau_i \|q^I\|_{I_i} \|\Gamma'\|_{1, I_i} \leq \frac{2\varepsilon_c}{\varepsilon_d (\mu_1 - \mu_0)} \max_{i=1, \dots, N} \tau_i \|q\|_{I_i},$$

by Theorem 1. Comparison with (17) suggests to choose the stabilisation parameters as follows.

$$(19) \quad \tau_i = \tau^* \frac{\varepsilon_d (\mu_1 - \mu_0) \gamma^*}{\varepsilon_c} \min \left\{ \frac{h_i^2}{8\varepsilon_d}, \frac{h_i}{2\varepsilon_c \|b\|_{I_i}} \right\},$$

with some constant $\tau^* \geq 0$.

Remark 4. If $\varepsilon_c = 1$ then $\varepsilon_d (\mu_1 - \mu_0) \gamma^* \varepsilon_c^{-1} \leq C$ and (19) is the standard recommended choice for the streamline-diffusion parameter from the literature, see e.g. [20].

Collecting (15)-(18), we arrive at our main result.

Theorem 2. *Suppose (2) is satisfied. Let the stabilisation parameters be chosen according to (19). Then the error of the SDFEM (12) satisfies*

$$\|u - u^N\| \leq \eta_1 + \eta_2,$$

where $\eta_k := \max_{i=1, \dots, N} \eta_{k,i}$, $k = 1, 2$,

$$\eta_{1,i} := \|q - q^I\|_{I_i} \quad \text{and} \quad \eta_{2,i} := (1 + 2\tau^*)\gamma^* \|q^I\|_{I_i} \min \left\{ \frac{h_i^2}{8\varepsilon_d}, \frac{h_i}{2\varepsilon_c \|b\|_{I_i}} \right\}.$$

Remark 5. *The error has been bounded in terms of the numerical solution u^N and of the data of the problem. The first part of the error bound can be further expanded using (14):*

$$(20) \quad \eta_{1,i} \leq \|f - f^I\|_{I_i} + \|cu^N - (cu^N)^I\|_{I_i} + \varepsilon_c \|b - b^I\|_{I_i} \frac{|u_i^N - u_{i-1}^N|}{h_i}$$

Apparently, sampling of the data is inevitable. However, instead of sampling (20) it seems advisable to directly sample $\eta_{1,i}$:

$$(21) \quad \eta_{1,i} \approx \tilde{\eta}_{1,i} := \left| (q - q^I)_{i-1/2} \right| = \frac{1}{2} |q_i^- - 2q_{i-1/2} + q_{i-1}^+|.$$

This avoids the use of a triangle inequality and therefore gives in general sharper upper bounds for the error. Note that the additional errors introduced in (21) are of higher order and decay rapidly when the mesh is refined.

5. An adaptive algorithm

We shall now consider a simple mesh movement algorithm, originally due to de Boor [5], which starts with a uniform mesh and aims to construct a mesh that solves the following equidistribution problem

$$(22) \quad M_i h_i = \frac{1}{N} \sum_{j=1}^N M_j h_j \quad \text{for } i = 1, \dots, N,$$

where we choose the monitor function $M = M(u^N, \bar{\omega}_N)$ in the algorithm from the *a posteriori* error estimate of Theorem 2 and Remark 5:

$$M_i := \sqrt{\tilde{\eta}_{1,i} + \eta_{2,i}}.$$

Note. Taking the square root here is essential because the method is of second order.

The equidistribution principle (22) does not need to be enforced strictly. The de Boor algorithm we are going to describe now can be stopped when the weakend equidistribution principle

$$M_i h_i \leq \frac{C_0}{N} \sum_{j=1}^N M_j h_j \quad \text{for } i = 1, \dots, N,$$

with a user-chosen constant $C_0 > 1$ is satisfied. We will see that $C_0 = 1.1$ produces suitable layer-adapted meshes and requires quite few iterations.

Algorithm:

1. Initialisation: Fix N and choose the constant $C_0 > 1$. The initial mesh $\bar{\omega}_N^{(0)}$ is uniform with mesh size $1/N$.
2. For $k = 0, 1, \dots$, given the mesh $\bar{\omega}_N^{(k)}$, compute the discrete solution $u^{N,(k)}$ by means of the SDFEM (12) on this mesh. Set $h_i^{(k)} = x_i^{(k)} - x_{i-1}^{(k)}$ for each i . Let the piecewise-constant monitor function $\tilde{M}^{(k)}$ be defined by

$$\tilde{M}^{(k)}(x) := M_i^{(k)} := M_i \left(u^{N,(k)}, \bar{\omega}_N^{(k)} \right) \quad \text{for } x \in (x_{i-1}^{(k)}, x_i^{(k)})$$

Then the total integral of the monitor function $M^{(k)}$ is

$$J^{(k)} := \int_0^1 \tilde{M}^{(k)}(x) \, dx = \sum_{i=1}^N M_i^{(k)} h_i^{(k)}.$$

3. Test mesh: If

$$(23) \quad \max_{i=1, \dots, N} M_i^{(k)} h_i^{(k)} \leq C_0 J^{(k)} N^{-1},$$

then go to Step 5. Otherwise, continue to Step 4.

4. Generate a new mesh by equidistributing the monitor function $\tilde{M}^{(k)}$ of the current computed solution: Choose the new mesh $\bar{\omega}_N^{(k+1)}$ such that

$$\int_{I_i^{(k+1)}} M^{(k)}(x) \, dx = J^{(k)} / N, \quad i = 0, \dots, N.$$

(Since $\int_0^x M^{(k)}(t) \, dt$ is increasing in x , the above relation clearly determines the $x_i^{(k+1)}$ uniquely.) Return to Step 2.

5. Set $\bar{\omega}_N^* = \bar{\omega}_N^{(k)}$ and $u^{N,*} = u^{N,(k)}$ then stop.

Remark 6. *This algorithm with an arc-length monitor function, i.e., with*

$$M_i = \sqrt{\alpha + \frac{(u_{i+1}^N - u_i^N)^2}{h_{i+1}^2}}, \quad \alpha = \text{const} > 0,$$

was applied to singularly perturbed problems by Beckett and Mackenzie [3, 4] and by Kopteva and Stynes [13]. For an inverse monotone 1st-order upwind difference scheme and $\varepsilon_c = 1$, the algorithm is studied in detail in [13]. The stopping criteria is shown to be met after $\mathcal{O}(1/\varepsilon_d)$ iterations. Chandra and Kopteva [6] analyse the de Boor algorithm applied to central differencing for a reaction-diffusion problem ($\varepsilon_c = 0$).

No attempt has been made yet to analyse the above algorithm for the SDFEM applied to the general reaction-convection-diffusion problem (1).

6. Numerical results

We now consider the test problem

$$(24) \quad -\varepsilon_d u''(x) - \varepsilon_c u'(x) + u(x) = e^{1-x}, \quad \text{for } x \in (0, 1), \quad u(0) = u(1) = 0$$

in order to illustrate the results of our theoretical findings and to study numerically the magnitude of the two components of our error estimator. We shall also verify how sharp the *a posteriori* error estimate is. The streamline-diffusion stabilisation is chosen according to (19) with $\tau^* = 1$.

The exact solution of (24) is easily computed, however the continuous maximum norm of the error has to be approximated. Let $\tilde{\omega}_N$ be the mesh obtained by three

N	χ^N	p^N	$\tilde{\eta}_1^N$	η_2^N	η^N	π^N	ϱ^N
2^{10}	6.45e-05	2.00	2.87e-06	3.07e-04	3.10e-04	2.00	4.80
2^{11}	1.61e-05	2.00	7.18e-07	7.68e-05	7.75e-05	2.00	4.80
2^{12}	4.03e-06	2.00	1.80e-07	1.92e-05	1.94e-05	2.00	4.80
2^{13}	1.01e-06	1.99	4.49e-08	4.80e-06	4.85e-06	2.00	4.80
2^{14}	2.54e-07	1.97	1.12e-08	1.20e-06	1.21e-06	2.00	4.76
2^{15}	6.49e-08	1.94	2.81e-09	3.00e-07	3.03e-07	2.00	4.67
2^{16}	1.69e-08	1.98	7.02e-10	7.50e-08	7.57e-08	2.00	4.48
2^{17}	4.29e-09	2.00	1.75e-10	1.88e-08	1.89e-08	2.00	4.41
2^{18}	1.07e-09	2.00	4.39e-11	4.69e-09	4.73e-09	2.00	4.41
2^{19}	2.68e-10	2.00	1.10e-11	1.17e-09	1.18e-09	2.00	4.41
2^{20}	6.71e-11	—	2.74e-12	2.93e-10	2.96e-10	—	4.41

TABLE 1. The SDFEM for (24) on a Bakhvalov mesh, $\varepsilon_d = 10^{-8}$, $\varepsilon_c = 10^{-3}$.

N	χ^N	p^N	$\tilde{\eta}_1^N$	η_2^N	η^N	π^N	ϱ^N
2^{10}	3.73e-03	1.72	1.24e-06	2.55e-02	2.55e-02	1.63	6.83
2^{11}	1.13e-03	1.75	3.09e-07	8.25e-03	8.25e-03	1.80	7.30
2^{12}	3.37e-04	1.77	7.69e-08	2.37e-03	2.37e-03	1.76	7.03
2^{13}	9.88e-05	1.79	1.91e-08	6.98e-04	6.98e-04	1.78	7.07
2^{14}	2.86e-05	1.80	4.77e-09	2.03e-04	2.03e-04	1.80	7.09
2^{15}	8.22e-06	1.81	1.19e-09	5.84e-05	5.84e-05	1.81	7.10
2^{16}	2.34e-06	1.83	2.95e-10	1.66e-05	1.66e-05	1.82	7.11
2^{17}	6.60e-07	1.84	7.35e-11	4.69e-06	4.69e-06	1.83	7.11
2^{18}	1.85e-07	1.84	1.83e-11	1.32e-06	1.32e-06	1.84	7.11
2^{19}	5.15e-08	1.85	4.55e-12	3.66e-07	3.66e-07	1.85	7.11
2^{20}	1.43e-08	—	1.13e-12	1.02e-07	1.02e-07	—	7.11

TABLE 2. The SDFEM for (24) on a Shishkin mesh, $\varepsilon_d = 10^{-8}$, $\varepsilon_c = 10^{-3}$.

times bisecting $\bar{\omega}_N$. Hence, we put an extra seven, evenly distributed points in each of the intervals of $\bar{\omega}_N$. Then we approximate

$$\|u - u^N\| \approx \chi^N := \|u - u^N\|_{\bar{\omega}_N}.$$

In view of Remark 5 we use the error estimator $\eta^N := \tilde{\eta}_1^N + \eta_2^N$. The efficiency of the error estimator is evaluated by computing the quantities $\varrho^N := \eta^N / \chi^N$. We also estimate the rates of convergence using standard formulae:

$$p^N := \log_2(\chi^N / \chi^{2N}) \quad \text{and} \quad \pi^N := \log_2(\eta^N / \eta^{2N}).$$

6.1. Reaction-convection-diffusion. For our first experiments we take $\varepsilon_d = 10^{-8}$ and $\varepsilon_c = 10^{-3}$. Two layers of different widths form: one of width $\mathcal{O}(\varepsilon^{-5})$ at $x = 0$ and the other at $x = 1$ which is of width $\mathcal{O}(\varepsilon^{-3})$.

Table 1 contains the results of our test computations for a Bakhvalov mesh with parameters $\sigma_0 = \sigma_1 = 3$ and $K_0 = K_1 = 1$. With this choice approximately a quarter of the mesh points is used to resolve each of the two layers. The table lists, from left to right, the number N of mesh intervals, the maximum-norm error, the two components of the error estimator, the upper error bound of Theorem 2 and, finally, the efficiency index ϱ^N . The errors χ^N and the error estimates η^N behave like $\mathcal{O}(N^{-2})$.

In Table 2 we give results for a Shishkin mesh with $\sigma_0 = \sigma_1 = 3$ and $q_0 = q_1 = 1/4$. Again a quarter of the mesh points is used to resolve either layer. The

N	χ^N	p^N	$\tilde{\eta}_1^N$	η_2^N	η^N	π^N	ϱ^N	K^N
2^{10}	2.05e-05	2.02	1.32e-05	1.02e-04	1.15e-04	2.17	5.62	15
2^{11}	5.05e-06	1.94	2.19e-06	2.35e-05	2.57e-05	2.16	5.09	14
2^{12}	1.31e-06	1.96	2.69e-07	5.51e-06	5.77e-06	2.05	4.40	7
2^{13}	3.37e-07	1.81	1.32e-07	1.26e-06	1.40e-06	1.72	4.14	8
2^{14}	9.63e-08	1.76	8.00e-08	3.44e-07	4.24e-07	2.12	4.40	5
2^{15}	2.84e-08	1.73	1.39e-08	8.34e-08	9.73e-08	1.82	3.43	6
2^{16}	8.57e-09	1.99	5.66e-09	2.20e-08	2.76e-08	2.04	3.22	4
2^{17}	2.16e-09	1.97	1.51e-09	5.19e-09	6.70e-09	1.99	3.09	4
2^{18}	5.51e-10	1.98	4.98e-10	1.19e-09	1.69e-09	2.12	3.06	3
2^{19}	1.39e-10	1.99	1.25e-10	2.62e-10	3.87e-10	1.97	2.77	3
2^{20}	3.52e-11	—	3.64e-11	6.22e-11	9.86e-11	—	2.80	3

TABLE 3. The SDFEM with adaptive mesh movement for (24), $\varepsilon_d = 10^{-8}$, $\varepsilon_c = 10^{-3}$.

errors χ^N and η_2^N and η^N behave like $\mathcal{O}(N^{-2} \ln^2 N)$. In contrast $\tilde{\eta}_1^N$ behaves like $\mathcal{O}(N^{-2})$. It can be concluded that η_2^N is the dominant term in the error estimator.

Both for the Bakhvalov mesh and for the Shishkin mesh the efficiency index ϱ^N is moderate (≈ 5 and ≈ 7).

Next consider the adaptive algorithm of § 5 with $C_0 = 1.1$; see Table 3. The last column of the table contains the iteration count for the algorithm. The order of convergence is close to 2, while the efficiency index for the finest meshes is smaller than 3.

6.2. Convection-diffusion. Next, we chose $\varepsilon_d = 10^{-8}$ and $\varepsilon_c = 1$. This time only one layer of different width $\mathcal{O}(10^{-8})$ forms at $x = 0$. The parameters in the construction of the meshes are chosen as above when $\varepsilon_c = 10^{-3}$ was considered.

For the Bakhvalov mesh (Table 4), convergence of second order is observed as in the first test case. Also the two components $\tilde{\eta}_1^N$ and η_2^N are proportional to N^{-2} . In the case of the Shishkin mesh (Table 5), convergence is spoiled by the typical logarithmic factor. Again it turns out that η_2^N is the dominating part of the error estimator, while $\tilde{\eta}_1^N$ becomes negligible for large N .

Table 6 illustrates the effectiveness of the adaptive algorithm from §5 in the convection dominated regime.

N	χ^N	p^N	$\tilde{\eta}_1^N$	η_2^N	η^N	π^N	ϱ^N
2^{10}	1.27e-05	2.00	1.29e-06	6.05e-05	6.18e-05	2.00	4.87
2^{11}	3.17e-06	2.00	3.24e-07	1.51e-05	1.54e-05	2.00	4.87
2^{12}	7.92e-07	2.00	8.10e-08	3.78e-06	3.86e-06	2.00	4.87
2^{13}	1.98e-07	2.00	2.02e-08	9.46e-07	9.66e-07	2.00	4.87
2^{14}	4.95e-08	2.00	5.06e-09	2.36e-07	2.41e-07	2.00	4.88
2^{15}	1.24e-08	2.00	1.27e-09	5.91e-08	6.04e-08	2.00	4.88
2^{16}	3.10e-09	2.00	3.16e-10	1.48e-08	1.51e-08	2.00	4.88
2^{17}	7.74e-10	2.00	7.91e-11	3.69e-09	3.77e-09	2.00	4.87
2^{18}	1.94e-10	2.00	1.98e-11	9.23e-10	9.43e-10	2.00	4.87
2^{19}	4.84e-11	2.00	4.94e-12	2.31e-10	2.36e-10	2.00	4.87
2^{20}	1.21e-11	—	1.24e-12	5.77e-11	5.90e-11	—	4.87

TABLE 4. The SDFEM for (24) on a Bakhvalov mesh, $\varepsilon_d = 10^{-8}$, $\varepsilon_c = 1$.

N	χ^N	p^N	$\tilde{\eta}_1^N$	η_2^N	η^N	π^N	ϱ^N
2 ¹⁰	1.63e-03	1.72	7.29e-07	1.11e-02	1.11e-02	1.70	6.85
2 ¹¹	4.93e-04	1.75	1.82e-07	3.44e-03	3.44e-03	1.73	6.98
2 ¹²	1.47e-04	1.77	4.56e-08	1.03e-03	1.03e-03	1.76	7.05
2 ¹³	4.30e-05	1.79	1.14e-08	3.05e-04	3.05e-04	1.78	7.09
2 ¹⁴	1.25e-05	1.80	2.85e-09	8.87e-05	8.87e-05	1.80	7.11
2 ¹⁵	3.58e-06	1.81	7.12e-10	2.55e-05	2.55e-05	1.81	7.12
2 ¹⁶	1.02e-06	1.83	1.78e-10	7.26e-06	7.26e-06	1.82	7.13
2 ¹⁷	2.87e-07	1.84	4.45e-11	2.05e-06	2.05e-06	1.83	7.13
2 ¹⁸	8.06e-08	1.84	1.11e-11	5.75e-07	5.75e-07	1.84	7.13
2 ¹⁹	2.24e-08	1.85	2.78e-12	1.60e-07	1.60e-07	1.85	7.14
2 ²⁰	6.22e-09	—	6.95e-13	4.44e-08	4.44e-08	—	7.14

TABLE 5. The SDFEM for (24) on a Shishkin mesh, $\varepsilon_d = 10^{-8}$, $\varepsilon_c = 1$.

N	χ^N	p^N	$\tilde{\eta}_1^N$	η_2^N	η^N	π^N	ϱ^N	K^N
2 ¹⁰	4.87e-06	2.04	9.36e-06	1.61e-05	2.55e-05	2.02	5.22	14
2 ¹¹	1.19e-06	1.80	2.42e-06	3.86e-06	6.28e-06	1.91	5.29	14
2 ¹²	3.41e-07	2.19	6.17e-07	1.05e-06	1.67e-06	2.07	4.90	5
2 ¹³	7.47e-08	1.76	1.56e-07	2.43e-07	3.99e-07	1.90	5.34	13
2 ¹⁴	2.21e-08	1.86	3.92e-08	6.74e-08	1.07e-07	1.97	4.83	5
2 ¹⁵	6.07e-09	2.30	9.84e-09	1.75e-08	2.73e-08	2.05	4.50	5
2 ¹⁶	1.23e-09	1.90	2.46e-09	4.15e-09	6.61e-09	1.95	5.37	9
2 ¹⁷	3.30e-10	2.04	6.16e-10	1.09e-09	1.71e-09	2.06	5.18	4
2 ¹⁸	8.06e-11	1.99	1.54e-10	2.55e-10	4.09e-10	1.96	5.08	4
2 ¹⁹	2.02e-11	1.98	3.86e-11	6.69e-11	1.05e-10	2.05	5.21	6
2 ²⁰	5.14e-12	—	9.66e-12	1.58e-11	2.54e-11	—	4.95	6

TABLE 6. The SDFEM with adaptive mesh movement for (24), $\varepsilon_d = 10^{-8}$, $\varepsilon_c = 1$.

N	χ^N	p^N	$\tilde{\eta}_1^N$	η_2^N	η^N	π^N	ϱ^N	K^N
2 ¹⁰	2.90e-05	3.31	1.03e-05	1.95e-04	2.05e-04	0.82	7.09	100
2 ¹¹	2.93e-06	2.41	1.36e-06	1.15e-04	1.16e-04	3.86	39.70	100
2 ¹²	5.51e-07	1.41	4.14e-07	7.56e-06	7.98e-06	2.40	14.47	100
2 ¹³	2.08e-07	2.38	1.19e-07	1.39e-06	1.51e-06	3.16	7.25	100
2 ¹⁴	3.99e-08	1.89	2.00e-08	1.49e-07	1.69e-07	2.07	4.23	22
2 ¹⁵	1.08e-08	1.56	5.37e-09	3.48e-08	4.01e-08	2.02	3.72	3
2 ¹⁶	3.67e-09	1.93	1.53e-09	8.38e-09	9.91e-09	1.94	2.70	3
2 ¹⁷	9.65e-10	1.81	5.01e-10	2.09e-09	2.59e-09	1.85	2.68	3
2 ¹⁸	2.75e-10	1.90	1.99e-10	5.21e-10	7.19e-10	1.95	2.62	3
2 ¹⁹	7.38e-11	1.85	5.55e-11	1.30e-10	1.86e-10	1.84	2.52	3
2 ²⁰	2.04e-11	—	1.91e-11	3.26e-11	5.17e-11	—	2.53	2

TABLE 7. The SDFEM with adaptive mesh movement for (24), $\varepsilon_d = 10^{-8}$, $\varepsilon_c = 10^{-5}$.

6.3. Reaction-diffusion. Finally, we consider the case of small convection: $\varepsilon_d = 10^{-8}$ and $\varepsilon_c = 10^{-5}$. Two layers of different width $\mathcal{O}(10^{-4})$ form at both end points of the domain.

For both the Bakhvalov mesh and the Shishkin mesh, similar behaviour is observed as for the two other parameter regimes.

For the adaptive procedure, Table 7 illustrates difficulties for “small” values of N . The algorithm fails to meet the stopping criterion (23) within 100 iterations. This can be improved

N	χ^N	p^N	$\tilde{\eta}_1^N$	η_2^N	η^N	π^N	ϱ^N	K^N
2^{10}	1.21e-05	2.59	3.03e-06	6.57e-05	6.88e-05	1.81	5.68	8
2^{11}	2.01e-06	1.57	1.02e-06	1.86e-05	1.96e-05	2.19	9.77	4
2^{12}	6.76e-07	2.46	2.63e-07	4.02e-06	4.29e-06	1.77	6.34	4
2^{13}	1.22e-07	1.82	7.57e-08	1.18e-06	1.25e-06	2.71	10.22	3
2^{14}	3.48e-08	1.19	1.47e-08	1.76e-07	1.91e-07	1.47	5.49	3
2^{15}	1.52e-08	2.41	4.93e-09	6.39e-08	6.88e-08	2.48	4.52	2
2^{16}	2.87e-09	2.13	1.33e-09	1.10e-08	1.24e-08	2.09	4.30	2
2^{17}	6.58e-10	2.03	3.72e-10	2.54e-09	2.91e-09	2.03	4.43	2
2^{18}	1.61e-10	2.01	9.37e-11	6.19e-10	7.13e-10	2.00	4.43	2
2^{19}	4.00e-11	2.00	2.50e-11	1.54e-10	1.79e-10	2.00	4.46	2
2^{20}	1.00e-11	—	6.34e-12	3.82e-11	4.46e-11	—	4.46	2

TABLE 8. Modified monitor \hat{M}_i and relaxed equidistribution $C_0 = 1.5$.

- (a) by relaxing the equidistribution principle by choosing $C_0 = 1.5$ and
 - (b) by modifying the monitor and use $\hat{M}_i := \sqrt{h_i^2 + \tilde{\eta}_{1,i} + \eta_{2,i}}$ instead of M_i .
- Incorporating the local mesh sizes yields a damping of the mesh movement.

The effect of these modifications, i.e. fewer iterations, is illustrated by the numbers in Table 8.

Acknowledgments

This publication has emanated from research conducted with the financial support of Science Foundation Ireland under the Research Frontiers Programme 2008; Grant 08/RFP/MTH1536 (PI N. Kopteva, University of Limerick). The author also acknowledges support from the Czech Academy of Sciences through their visiting scholar programme.

References

- [1] M. Ainsworth, J. T. Oden. *A posteriori error estimation in finite element analysis*, Wiley, Chichester, 2000.
- [2] N. S. Bakhvalov. Towards optimisation of methods for solving boundary value problems in the presence of boundary layers. *Zh. Vychisl. Mat. i Mat. Fiz.*, 9:841–859, 1969. in Russian.
- [3] G. Beckett. *The robust and efficient numerical solution of singularly perturbed boundary value problems using grid adaptivity*. Ph. D. thesis, University of Strathclyde, Glasgow, 1999.
- [4] G. Beckett, J. Mackenzie. Convergence analysis of finite difference approximations on equidistributed grids to a singularly perturbed boundary value problem. *Appl. Numer. Math.* 35(2):87–109, 2000.
- [5] C. de Boor. *Good Approximation by Splines with Variable Knots II*. Lecture Notes in Mathematics, volume 363. Springer, Berlin, 1973.
- [6] N. M. Chadha, N. Kopteva. A robust grid equidistribution method for a one-dimensional singularly perturbed semilinear reaction-diffusion problem. *IMA J. Numer. Anal.*, in press.
- [7] N. M. Chadha, N. Kopteva: Maximum norm a posteriori error estimate for a 3d singularly perturbed semilinear reaction-diffusion problem, submitted.
- [8] J. L. Gracia, E. O’Riordan, and M. L. Pickett. A parameter robust second order numerical method for a singularly perturbed two-parameter problem. *Appl. Numer. Math.*, 56(7):962–980, 2006.
- [9] T. J. R. Hughes and A. Brooks. A multidimensional upwind scheme with no crosswind diffusion. In T. J. R. Hughes, editor, *Finite Element Methods for Convection Dominated Flows*, pages 19–35. AMD. Vol. 34, ASME, New York, 1979.
- [10] Kopteva, N.: Maximum norm a posteriori error estimates for a one-dimensional convection-diffusion problem. *SIAM J. Numer. Anal.*, 39(2):423–441, 2001.
- [11] N. Kopteva. Maximum norm a posteriori error estimates for a 1D singularly perturbed semilinear reaction-diffusion problem. *IMA J. Numer. Anal.*, 27(3):576–592, 2007.
- [12] N. Kopteva. Maximum norm a posteriori error estimate for a 2D singularly perturbed reaction-diffusion problem. *SIAM J. Numer. Anal.*, 46(3):1602–1618, 2008.

- [13] N. Kopteva, M. Stynes. A robust adaptive method for a quasi-linear one-dimensional convection-diffusion problem. *SIAM J. Numer. Anal.* 39(4):1446–1467, 2001.
- [14] T. Linß. Layer-adapted meshes for one-dimensional reaction-convection-diffusion problems. *J. Numer. Math.*, 12(3):193–205, 2004.
- [15] T. Linß. *Layer-adapted meshes for reaction-convection-diffusion problems*. Lecture Notes in Mathematics, volume 1985. Springer, Berlin, 2009.
- [16] T. Linß. Maximum-norm error analysis of a non-monotone FEM for a singularly perturbed reaction-diffusion problem. *BIT*, 47(2):379–391, 2007.
- [17] T. Linß and H.-G. Roos. Analysis of a finite-difference scheme for a singularly perturbed problem with two small parameters. *J. Math. Anal. Appl.*, 289(2):355–366, 2004.
- [18] J. J. H. Miller, E. O’Riordan, and G. I. Shishkin. *Fitted numerical methods for singular perturbation problems. Error estimates in the maximum norm for linear problems in one and two dimensions*. World Scientific, Singapore, 1996.
- [19] M. H. Protter and H. F. Weinberger. *Maximum principles in differential equations*. Springer-Verlag, Berlin, Heidelberg, 1984.
- [20] H.-G. Roos, M. Stynes, and L. Tobiska. *Robust Numerical Methods for Singularly Perturbed Differential Equations*, volume 24 of *Springer Series in Computational Mathematics*. Springer, Berlin, 2nd edition, 2008.
- [21] H.-G. Roos and Z. Uzelac. The SDFEM for a convection-diffusion problem with two small parameters. *Comput. Meth. Appl. Math.*, 3(3):443–458, 2003.
- [22] G. I. Shishkin and V. A. Titov. A difference scheme for a differential equation with two small parameters at the derivatives. *Numer. Meth. Cont. Med. Mechanics*, Novosibirsk, 7(2):145–155, 1976.
- [23] R. Verfürth: *A Review of a posteriori error estimation and adaptive mesh-refinement techniques*, Wiley-Teubner, 1996.
- [24] R. Verfürth: Robust a posteriori error estimates for stationary convection-diffusion equations, *SIAM J. Numer. Anal.* 43(4):1766–1782, 2005.

Institut für Numerische Mathematik, Technische Universität Dresden, D-01062 Dresden, Germany

E-mail: torsten.linss@tu-dresden.de.

URL: <http://www.math.tu-dresden.de/~torsten/>